Pergamon

Cement and Concrete Research, Vol. 26, No. 1, pp. 63-68, 1996

0008-8846/96 $15.00 + .00

0008-8846(95)00180-8

EFFECTS OF SILICA FUME AND AGGREGATE SIZE ON THE BRITTLENESS OF CONCRETE

Canan Tasdemir, Mehmet A. Tasdemir
Faculty of Civil Engineering, Istanbul Technical University, Istanbul, Turkey

Frank D. Lydon and Ben I.G. Barr
Division of Civil Engineering, University of Wales Cardiff, U.K.

(Communicated by A.J. Majundar)
(Received September 26, 1995)

ABSTRACT

The effects of silica fume and aggregate size on the softening response and brittleness of high strength concretes were investigated by measuring the fracture energy G_F, the characteristic length l_{ch} and brittleness index B. Based on the fracture tests and microscopic studies at the aggregate-matrix interface, it was concluded that, in concretes without silica fume, the cement-aggregate interface had a profusion of calcium hydroxide and also much less dense calcium silicate hydrate, hence, the cracks usually developed at this weak interface, i.e. around coarse aggregate. However, in concretes with silica fume, the interfacial zone became stronger, more homogeneous and dense, hence, the cracks usually traversed the aggregates; transgranular type of fracture was observed. In these concretes, the fracture energy decreased dramatically especially for large size of aggregate case and as a result the brittleness index increased significantly.

Introduction

There is a growing interest in the study of aggregate-matrix interfaces (1-8). Since the interface between the aggregates and cement paste is the weakest link, the mechanical behaviour of concrete is significantly affected by the properties of the interfacial zone; the fracture of concrete is very sensitive to the properties of this zone (1-4). Previous studies on the fracture and microstructure of this region in normal strength concrete have led to some useful information, however more research and quantitative measurements are needed for the better understanding of high strength concretes with and without silica fume. In particular, a more realistic approach is required to investigate real concrete behaviour instead of mortar containing model aggregate. The effect of maximum size of aggregate on the fracture energy G_F is important because the crack surface roughness induces aggregate interlock (9).

The main objective of this work is to investigate the influence of silica fume replacement of cement and aggregate size on the brittleness of high strength concrete by determining some

TABLE 1
Mix Proportions of Concretes with and without Silica Fume

Mix Code	NC10	SC10	NC20	SC20
Cement content (kg/m^3)	402	365	404	367
Silica fume (SF) content (kg/m^3)	0	37	0	37
Sand (kg/m^3)	732	732	737	737
Coarse aggregate (kg/m^3) 5-10 mm	1098	1098	—	—
10-20mm	—	—	1105	1105
Superplasticizer (kg/m^3)	4.0	5.0	2.0	3.5
Water (kg/m^3)	146	146	147	147
W/(C+(SF)	0.36	0.36	0.36	0.36
SF/C	0	0.10	0	0.10
Air content (%)	2.8	2.4	2.4	2.0
Slump (mm)	60	60	80	60
Density of Fresh Concrete (kg/m^3)	2382	2382	2395	2397

fracture parameters such as fracture energy G_F(10), characteristic length(11) and also brittleness index(12-14). The effects of aggregate size and silica fume on the shape of the descending branch in the curves of load-CMOD (Crack Mouth Opening Displacement) and load-displacement at mid-span were supported by microstructural studies of the aggregate-cement paste interface and fracture surfaces.

Experimental Details

Four different high strength concrete batches with constant water/cement (or water/cement + silica fume) ratio were prepared from the same Portland cement and natural sand. Two different sizes of crushed limestone coarse aggregate (5-10 mm or 10-20 mm) were used in the study. For each maximum aggregate size, two different concretes one with and one without silica fume were cast. The silica fume (in slurry form and with 96.6 percent SiO_2 content) was 10 percent by weight of cement. The water/binder ratio was kept at 0.36 in all four concretes and a sodium naphthalene sulfonate type superplasticizer was used for all mixes. All concretes had the same nominal slump (60 mm to 80 mm). The concrete mixes were designated with the following code: NC10, SC10, NC20 and SC20. Concretes without and with silica fume were named NC and SC, respectively; the number following NC and SC shows the maximum aggregate size. Table 1 shows the mix proportions and some properties of fresh concretes. The specimens were cured in water, saturated with lime, for 27 days. At least three specimens of each concrete mix were tested under each type of loading condition at 28 days. The beams prepared for the RILEM fracture energy tests were 840 mm in length and 100 mm x 100 mm in cross-section. For the standard compressive and splitting tests, six 100 mm cubes were prepared.

TABLE 2
Properties of Hardened Concrete

Mix Code	NC10	SC10	NC20	SC20
Cube compressive strength, N/mm^2	72.7	87.5	72.0	84.5
Splitting tensile strength f_t, N/mm^2	4.58	5.42	3.45	4.03
Modulus of Elasticity E, kN/mm^2	38.0	37.5	37.2	37.0
Fracture energy G_F, N/m	106	87	142	87
Characteristic length l_{ch}, mm	192	111	444	198
Net bending stress, N/mm^2	5.28	5.78	4.49	5.45
Final displacement at mid-span δ_0, mm	0.913	0.760	1.337	0.930
Final CMOD, mm	0.470	0.383	0.650	0.395
Brittleness index B (S_{II}/S_I)	0.97	1.64	0.89	2.69

Test Procedure

The test for the determination of fracture energy, G_F, was performed according to the recommendation of the RILEM 50-FMC Technical Committee(10). The effective cross-section, however, was reduced to 60 mm x 100 mm by means of a saw cut and the length of the support span was 800 mm. The notched beam specimen tested is shown in the inset in Figure 1. During the test, load versus CMOD and load versus displacement at the mid-span were recorded. The details of the test method can be found in references (10) and (11). The static moduli of elasticity E were calculated from the load-CMOD curve using the initial compliance as described in reference (15). The splitting tensile strengths and compressive strengths were determined on 100 mm cubes. The characteristic length of the material, l_{ch}, which indicates its brittleness, is given by the expression:

$$l_{ch} = EG_F/f^2_t \quad (1)$$

where f_t is the tensile strength, obtained from the cube splitting tests.

The brittleness index B, found from loading/unloading each specimen in bending, is defined as the ratio of the elastic deformation energy to the irreversible deformation energy corresponding to the pre-peak point of the load-displacement at mid span curve(12-14). As shown in the inset in Figure 1, the brittleness index may be expressed as follows:

$$B = \text{area}S_{II}/\text{area}S_I \quad (2)$$

where S_I is the irreversible deformation energy due to damage and S_{II} is the elastic (reversible) deformation energy. As seen in Figure 1, when the ratio S_{II}/S_I approaches zero, all energies become irreversible; when it tends to infinity all energies become reversible. Table 2 summarises the test results obtained for the four concretes.

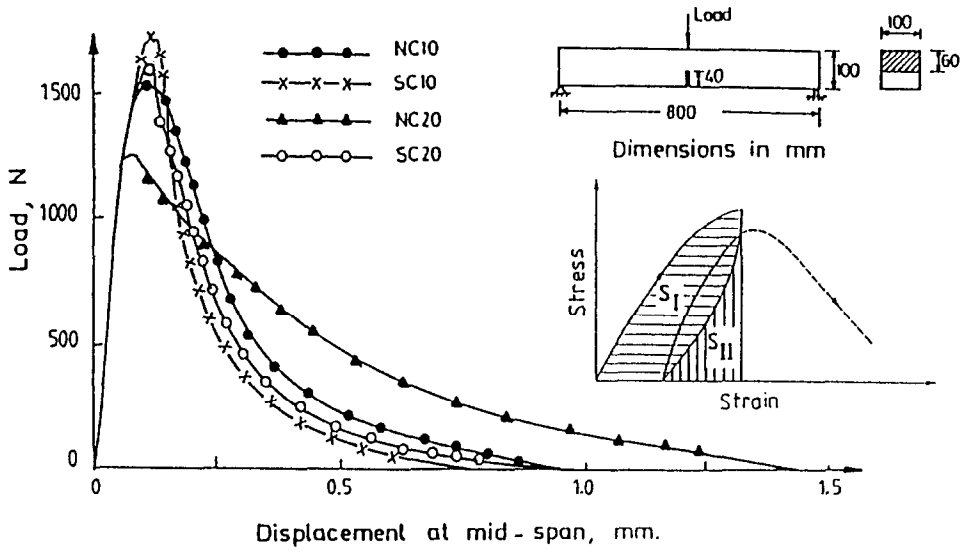

FIG. 1.
Typical results of load displacement at mid-span curves obtained from three point bending test.

Results and Discussion

As shown in Figure 1 the initial slopes of the load-displacement at mid-span curves for all four concretes are practically identical. However, there are significant effects of both aggregate size and silica fume replacement on the strength and especially on descending branches of all curves.

In concretes without silica fume, as shown in Figure 1, the softening response of NC20 has a longer tail than that of NC10, due to the aggregate bridging size. It can be concluded that the amount of crack bridging is determined by the maximum size of the aggregates and that longer tail is an indication of enhanced cracking both in size and number. van Mier(16) has also reported similar conclusions. As shown in Table 2, the fracture energy of concrete G_F and characteristic length l_{ch} strongly depend on the maximum aggregate size; both G_F and l_{ch} increase as the aggregate size increases.

Concretes with silica fume have a greater peak load and a steeper gradient of the softening branch with the corresponding lower final displacement values. Reduction in both G_F and l_{ch} and substantial increase in the brittleness number are also typical for these concretes; the characteristic length of SC20 concrete is less than half that of the NC20 concrete and brittleness index in SC20 is significantly high. Thus, in concretes with silica fume, the characteristic length decreases and the material becomes more brittle.

After completion of the bending tests the fracture surfaces were examined using both a stereo microscope, scanning electron microscope (SEM) and Energy Dispersive X-Ray Analizers (EDX). In concretes with silica fume, the cracks usually traversed through the aggregate; transgranular type of fracture was observed, and it was brittle in nature. In concretes without silica fume, however, the cracks usually developed around the coarse aggregate resulting in a more tortuous fracture path.

In concretes without silica fume the observation of abundant calcium hydroxide (CH) crystals at the paste-aggregate interface corresponds well with those of others(17-20). Apart from CH, some platy mono-sulphate (AFm) crystals were also identified in this region. Platy AFm and tabular CH crystals were also identifiable in the paste. The air voids were full of platy CH crystals.

In concretes with silica fume the interfacial zone was composed of dense C-S-H. The air voids in this region were empty and showed no deposition of CH, AFm and ettringite crystals. Dense paste identical to that of the interfacial zone was observed. As in the transion zone, the air voids in the paste were empty.

Conclusions

In the light of the experimental measurements, examinations of the fracture surfaces and the microstructural studies of the aggregate-matrix interfaces, the following conclusions can be drawn:

1. In concretes without silica fume with 20mm maximum size of aggregate, the descending branch of the load-displacement curve decreases slowly and a longer tail is observed. However, in concretes with silica fume, a steeper gradient of the softening branch with a shorter tail can be obtained for both 10 mm and 20 mm aggregates and the descending branches are nearly identical.
2. In concretes without silica fume the fracture energy and characteristic length strongly depend on the maximum size of aggregate. Both parameters increase as the aggregate size increases. In concretes with silica fume, the fracture energy and especially characteristic length decrease dramatically, brittleness increases significantly especially for 20mm maximum size of aggregate and the fracture energy G_F takes the same value for both maximum size of aggregates.
3. In concretes with silica fume, the cracks usually travel through the aggregate and fracture tends to be brittle in nature. In concretes without silica fume, however, the cracks usually develop around the coarse aggregate resulting in a more tortuous fracture path. This different crack pattern can be attributed to the interfacial zone becoming stronger and more homogeneous, as a result of silica fume inclusion, and the material exhibits a more brittle behaviour and transgranular type of fracture.

Acknowledgement

This research was done at the University of Wales Cardiff. The second author wishes to acknowledge the financial support from TÜBİTAK (The Scientific and Technical Research Council of Turkey) and The Royal Society for doing research at Cardiff in the European Science Exchange Programme. The help of Dr. S.L. Sarkar, S.E.C.A., Inc., Consulting Engineers, Houston, U.S.A., during the microstructural studies, is gratefully acknowledged.

References

1. S. Mindess and S.P. Shah (Eds.), Bonding in Cementitious Composites, Proc. Sym., MRS, Pittsburgh, (1988).

2. M. Maso (Ed.), Interfaces in Cementitious Composites, Proc. Int. Conf., Toulouse, E. and F.N. Spon, London, (1992).
3. P. Shah and M.A. Tasdemir, in Advances in Concrete Technology, V.M. Malhotra, ed., CANMET, Ottawa, Second Edition, 161 (1994).
4. M.A. Tasdemir, A.K. Maji and S.P. Shah, J. Engrg. Mech., ASCE, 116, 1058 (1990).
5. Mindes, S., in Materials Science of Concrete I, I, J.P. Skalny, Ed., Am. Ceram. Soc. (1989).
6. A. Goldman and A. Bentur, ACI Mater. J., 86, 440, (1989).
7. P.J.M. Monteiro and P.K. Metha, Cem. Concr. Res., 15, 378 (1985).
8. J.A. Larbi, Heron, Delft, 38, 1, (1993).
9. B.L. Karihaloo, Fracture Mechanics and Structural Concrete, Longman Group Ltd., Essex, (1995).
10. RILEM 50-FMC, Mater. Struct., 18, 285 (1985).
11. A. Hillerborg, Mater. Struct.18, 291 (1985).
12. K. Wu and J. Zhou, in Bonding in Cementitious Composites, S. Mindes and S.P. Shah, eds., MRS, Pittsburgh, 29 (1988).
13. E. Siebel, Darmstadt Concr., 3, 179 (1988).
14. C. Tasdemir, Microstructural Effects on the Mechanical Behaviour of High Strength Concretes, PhD Thesis, Ist. Tech. Univ., Istanbul, 1995.
15. RILEM TC 89-FMT, Mater. Struct., 23, 459 (1990).
16. J.G.M. van Mier, Cem. Concr. Res., 21, 1 (1991).
17. J.P. Skalny (Ed.), Materials Science of Concrete I, Am. Ceram. Soc. (1989).
18. S.L. Sarkar, in Advances in Concrete Technology, V.M. Malhotra, ed., CANMET, Ottawa, Second Edition, 125 (1994).
19. C. Tasdemir, S.L. Sarkar, M.A. Tasdemir, S. Akyüz and C. Koca, in Proc. ERMCO 95, Istanbul, 444 (1995).
20. C. Tasdemir, M.A. Tasdemir, R. Grimm and G. König, in FRAMCOS-2:2nd Int. Conf. Frac. Mech. Concr. and Concr. Struct., F.H. Wittmann, ed., Aedificatio Publishers, Freiburg, 1, 125, (1995).